Piezoelectric polyimide scanning micromirror

MAJ Paul Patterson[A], Dr. Madan Dubey[B], Jeffrey Pulskamp[B], Ronald Polcawich[B], Luke Currano[B], Dr. Jason Zara[C]

[A]U.S. Military Academy

West Point, New York

[B]Sensors and Electron Devices Directorate

U.S. Army Research Laboratory

Adelphi, Maryland

[C] The George Washington University,

Washington, DC

Executive Summary

This paper provides an overview of recent research in the use of microelectromechanical systems (MEMS) actuators for optical beam steering applications, including optical coherence tomography (OCT). In the past, prototype scanning devices have been fabricated out of polyimide substrates using conventional MEMS processing technology. The material properties of the polyimide allow very large scan angles to be realized in the devices. The prototype devices utilize piezoelectric bimorphs to mechanically actuate the torsion mirror. Using equipment at the Army Research Lab's Adelphi location these devices were characterized to allow for better modeling of the devices. Analytical models have been developed that predict the resonant frequency of the devices. Further finite element modeling (FEM) has been done using ANSYS. These models closely reflect the measured resonant frequencies of the prototype devices as well as their harmonic behavior. Based upon these models, further refinements have been made to the design to produce specific resonant frequencies for use in a multitude of applications. These refined FEM models were used to design new scanning devices which can be manufactured on a single wafer. Masks for the new devices have already been made. These devices are currently being fabricated on a single wafer with minimal post processing requirements at the Army Research Labs using thin film piezoelectric processing techniques. These new devices will operate at resonant frequencies between 20-50Hz which make them ideally suited for use in applications where real time imaging is desired.

1. Introduction

The field of optical MEMS or MOEMS has seen an explosive growth over the last few years. This growth is expected to continue for the foreseeable future. Emerging Opportunities in Optical MEMS: 2003-2007, a report from the Communications Industry Researchers, Inc. (CIR) states that the growth of MOEMS subsystems will grow from $560 million in 2003 to $1.7 billion in 2007 [1]. Numerous methods have been explored for beam steering applications in the field of MOEMS, and several categories have been developed to classify these micromirrors. For the purposes of this paper, micromirrors will be classified based upon their method of actuation. The various types of actuation techniques employed in the development of micromirrors can be roughly divided into one of three categories: electrostatic, electromagnetic, and piezoelectric [2]. A majority of micromirrors to date have relied on electrostatic actuation. In general, micromirrors that rely on electrostatic actuation require large drive voltages (>50V). Electrostatically actuated micro-mirrors have been fabricated that are capable of achieving rotational angels of 90°with drive voltages of 47V[3]. Other electrostatically actuated micromirrors have demonstrated scans of 21° at 3.6kHz with a driving voltage of 75 V[4]. Recently MEMs flexure PZT actuated scanners have been demonstrated which achieve optical angles of up to 40° in static operation and 10° in resonance at 17.4kHz [5]. Micromirrors, which utilize comb-drives for electrostatic actuation, have also been demonstrated. These devices are capable of 8.5° of mechanical deflection at 19.55kHz with an applied voltage of 100V [6]. Similar devices to those described in this paper have been fabricated out of polyimide and actuated electrostatically. These devices are capable of scanning up to 146° at 50V [7,8]. Most of the aforementioned devices operate at frequencies that are too high for use in real time medical imaging applications. Most utilize silicon hinges that are too stiff to achieve the large scan angles desired in medical imaging systems and other real time imaging systems. The processing required for many of the

aforementioned micromirror structures is very specialized and is not a viable means to mass produce such devices for use in medical imaging applications.

2. Methodology

2.1 Previous Work

In previous work, prototype scanning devices have been fabricated out of polyimide substrates using conventional patterning and etch techniques. The micromirror device is comprised of a table (with attached mirror) suspended by two small torsion hinges. These torsion hinges are fixed at one end to the supporting structure of the device. A gold-coated silicon mirror is then attached to the table of the device. **Figure 1** is a schematic of a prototype device without a mirror attached. No dimensions are given, as this is a general schematic that depicts the typical layout of any of the devices. **Figure 2** is an exploded view of the hinge structure. Initially 6 different prototype designs were fabricated. **Table 1** details the dimensions of these prototype devices.

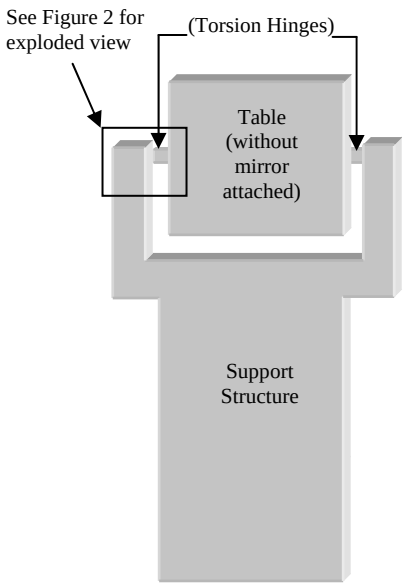

Figure 1: Schematic of polyimide support structure without mirror.

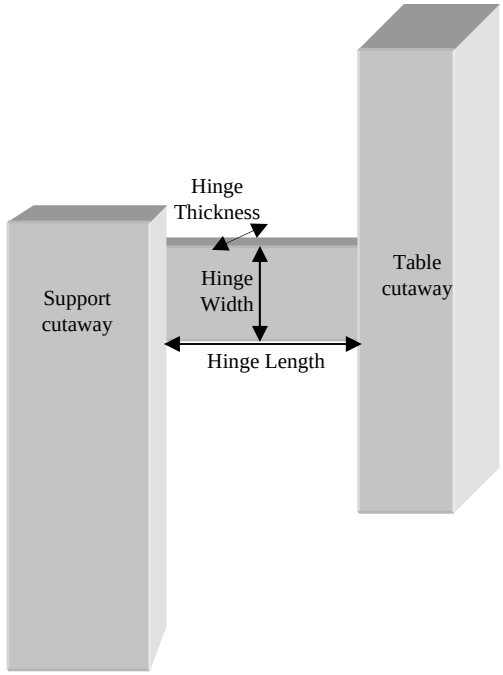

Figure 2: Exploded view of torsion hinge schematic.

Support Structure Size	Table Size (mm)	Hinge Width (μm)	Hinge Thickness (μm)	Hinge Length (μm)
Large	2 x 2.25	90	3	250
Large	2 x 2.25	135	3	250
Large	2 x 2.25	180	3	250
Small	1 x 1.125	60	3	250
Small	1 x 1.125	90	3	250
Small	1 x 1.125	120	3	250

Table 1: Table of different prototype devices and their dimensions.

Four different size gold coated silicon mirrors were fabricated for attachment to the six prototype devices ($0.875mm^2$, $1mm^2$, $1.5mm^2$, and $2mm^2$). The mirrors are all 400μm thick silicon wafers. **Figure 3** is a schematic of one of the larger prototype devices**.** F**igure 4** is a picture of an actual prototype device. The entire support structure of the device is made of polyimide. The mirrors are fabricated on a separate wafer of gold-coated single crystal silicon (400μm thick). The mass of the mirror and the dimensions of the hinges can be varied to develop devices with the desired scan deflections and frequency responses for a multitude of real time imaging applications.

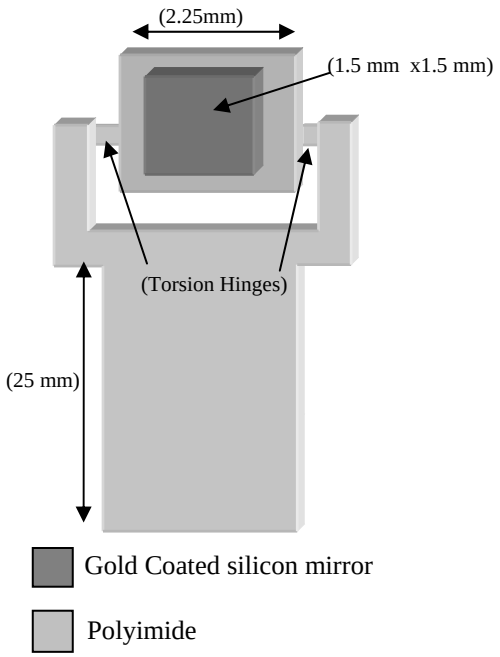

Figure 3: Schematic of torsion mirror device with a hinge width of 135μm and a mirror that is 1.5mm x 1.5mm.

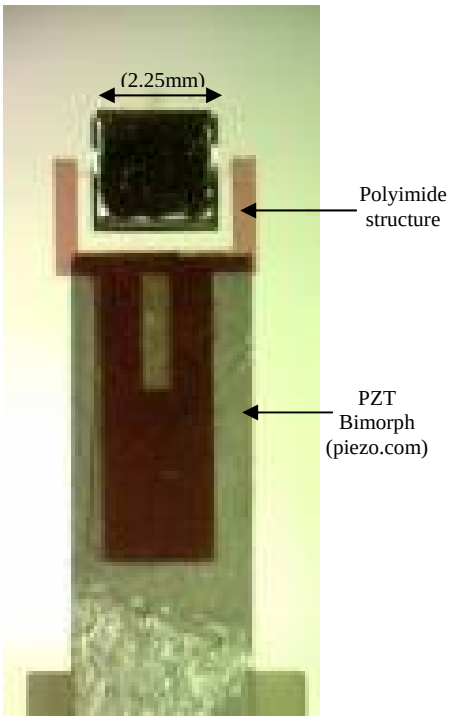

Figure 4: Picture of actual torsion mirror device with the same dimensions as those in **3**.

The initial prototype mirror assemblies were fabricated at North Carolina State University in the Biomedical Microsensors Laboratory (BMMSL) using a three-layer process on five-inch silicon wafers. A sacrificial silicon oxide layer was deposited on the wafer prior to processing to release the polyimide structures from the wafer. **Figure 5** shows several of the devices on a wafer prior to being released. This sacrificial layer was later etched away using hydrofluoric acid (HF). To form the thin hinge layer, a 3 μm layer of polyimide (PI-2723, HD Microsystems, Wilmington, DE) was spun onto the wafer and then patterned.

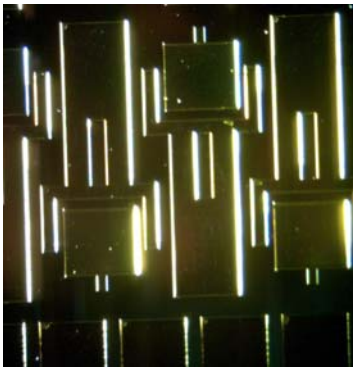

Figure 5: Picture of devices before being released from the wafer

Figures 6a and 6b show the cross section of this process and a top-down view. The thicker supports and tables were made of a 30μm thick patterned polyimide layer (Durimide, Arch Chemicals, Norwalk, CT). **See figures 6c and 6d**. The mirrors are made of gold plated single crystal silicon in a separate process on a separate wafer. Once the devices were released from the wafer using the HF etching solution, the mirrors were mounted. The mirrors were then glued to the polyimide table using a fast drying epoxy. The entire device is then mounted to the bimorph using double stick tape. This was a sufficient bonding method for testing purposes as the mass of the device was very small (less than 3mg).

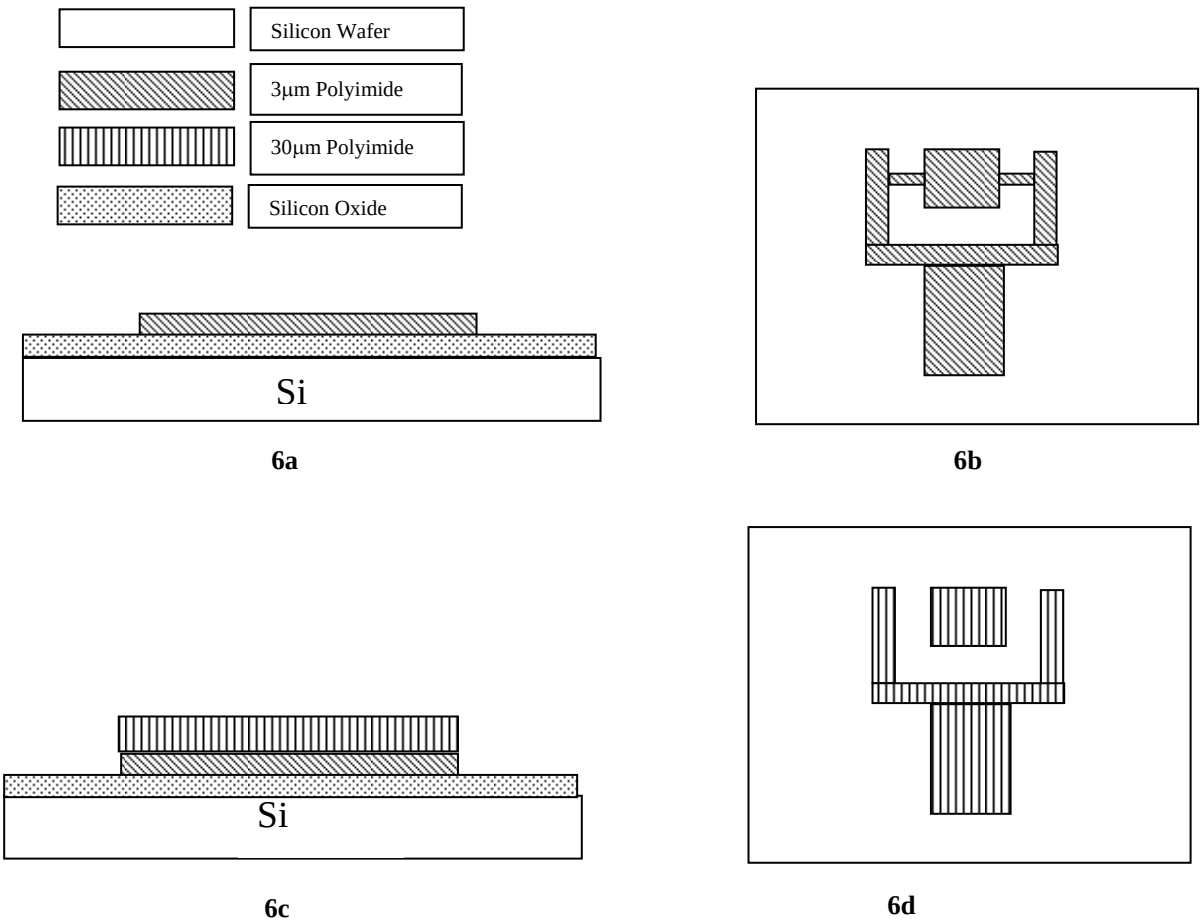

Figure 6: (a) Cross-section of mirror support structure with first layer of polyimide. **(b)** Top down view of first layer of polyimide. **(c)** Cross-section of second layer of polyimide for mirror support structure. **(d)** Top-down view of second layer of polyimide for mirror support structure.

2.2 Analytical and Theoretical Models

The mirror pivots about the torsion hinges when the whole structure is subjected to a forced vibration. This forced vibration is generated by a commercially purchased piezoelectric bimorph that is 2mm in width and 25mm in length (piezo.com) and is attached to the base of the prototype devices. The support structure of the prototype device has a relatively low resonant frequency (approximately 15-60Hz). This enables us to drive the entire structure at a frequency well below the bimorph resonant frequency of 215Hz. The small tip displacement of the bimorph at low voltages is enough to excite the device when operated at the device's resonance. The motion it causes in the polyimide structure amplifies the small tip displacement of the bimorph into a large optical scan angle.

Once in motion the mass of the mirror and its moment of inertia cause the hinges to twist. This develops a restoring torque in the hinges. The restoring torque is realized as the bimorph tip displaces in the opposite direction of travel. In a perfect oscillator this motion would continue indefinitely. However, in the case of our device there are numerous factors that cause the oscillating motion of the device to stop rather quickly when no force is applied. Operating the bimorph at the resonant frequency of the support structure allows us to overcome some of these effects. This forced vibration causes the device to behave more like a perfect torsional pendulum or oscillator.

The mirror and support structures can be modeled using one-dimensional beam theory and fundamental vibration mechanics. The resonant frequency of the structure can be predicted using equation 1 [9].

$$f_r = \frac{1}{2\pi}\sqrt{\frac{JG}{I\frac{l}{2}}} \qquad (1)$$

Where J is the polar moment of inertia of the hinge, G is the shear modulus of the hinge, I is the moment of inertia of the mirror, and l is the length of the hinge. The torque applied to the hinges causes a twisting motion. This motion is related to an angle in the hinge. The angle at which a hinge twists is the same angle that the mirror attached to the hinge is displaced. The angle of displacement can be predicted using equation 2.

$$\theta = \frac{TL}{JG} \qquad (2)$$

Where T is the torque applied, L is the length of the torsion hinge, J is the polar moment of inertia of the torsion hinge and G is the shear modulus. The torque is generated by the tip displacement of the piezoelectric bimorph accelerating the mass of the table and mirror.

MATLAB was used to develop analytical models for the device. These analytical models closely matched measured values in the prototype devices. The MATLAB models were then used to determine a range of acceptable hinge thicknesses and hinge widths to be used in the fabrication of new devices on a single wafer. **Table 2** shows the key material properties used to model the device.

Material	Modulus (GPa)	Density (kg/m^3)	Piezoelectric strain coefficient (d31)
Polyimide	2.5	1470	N/A
Silicon	160	2330	N/A
PZT	63	7500	1.8e-10 m/V

Table 2: Table of key material properties used for analytical models and ANSYS models.

Figure 7 shows a graph generated by MATLAB of the device resonant frequency versus the hinge width and hinge thickness. This graph was used to determine which device parameters met the frequency criteria for use in real time imaging applications (28-40Hz).

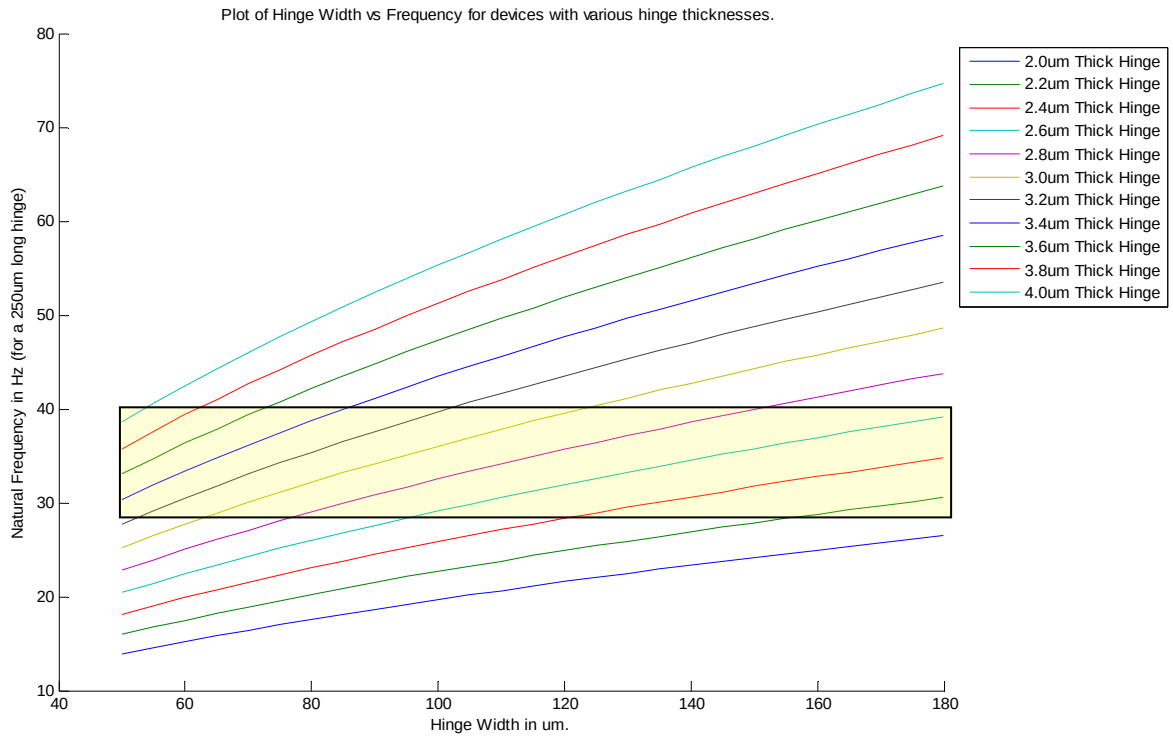

Figure 7: MATLAB graph of various hinge widths and thicknesses versus frequency. Note: the shaded rectangle shows our area of interest for real time imaging applications (28-40 Hz)

2.3 Finite Element Models (FEM)

The new devices were also modeled and simulated using a finite element analysis program (ANSYS, Inc., Canonsburg, PA). These simulations allowed us to further refine the parameters of the device to achieve the optimal resonant frequencies for use in imaging systems prior to manufacturing the devices. Previous attempts at modeling the devices in ANSYS yielded acceptable results but suffered from numerous unknown material properties. Using more specific material properties for the piezoelectric layer increased the accuracy of the FEM model. **Figure 8** shows the ANSYS modal analysis of a device with 135µm wide hinges.

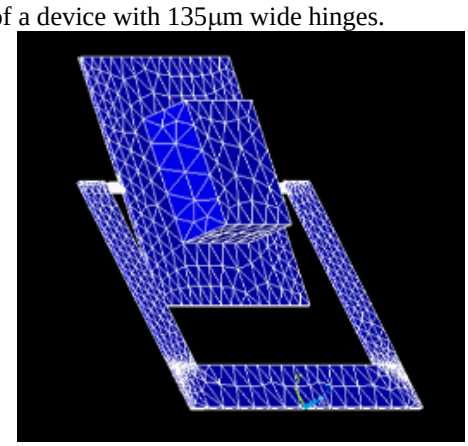

Figure 8: ANSYS modal animation of the device

Originally a volume mesh was used to generate the mesh for the modal analysis of the device. This was sufficient for modeling the prototype devices which consisted of polyimide and silicon materials. In order to model the entire device that would be fabricated on a single wafer and to conduct the harmonic analysis with the piezoelectric materials a more customized mesh was needed. The line and area mesh commands were used in the ANSYS batch file in order to assign different mesh granularities to regions of interest in the FEM model. The improved FEM model also allowed for a more accurate harmonic analysis of the device to be done. The harmonic analysis required a structural dampening ratio be given for the device. This value can be determined using the measured Q of the device as shown in equation 3 [10]. The Q was determined using Laser Doppler Vibrometry (LDV). The results of the LDV can be seen in **Figure 9**. Further measurements of the original prototype devices were conducted using a calibrated paper target and a HeNe laser. The corresponding scan angle of the device was then measured using the calibrated target. **Figure 10** shows a picture of the calibrated target with the HeNe laser being scanned across it.

$$\gamma = \frac{1}{2Q} \qquad (3)$$

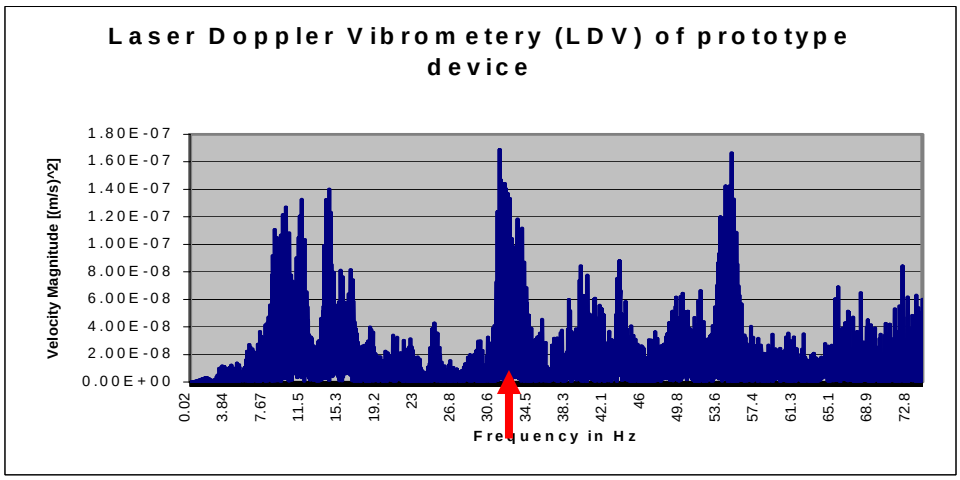

Figure 9: LDV of 135um hinge device with a drive voltage of 5Vp-p. Note the red arrow indicates the device's primary resonance.

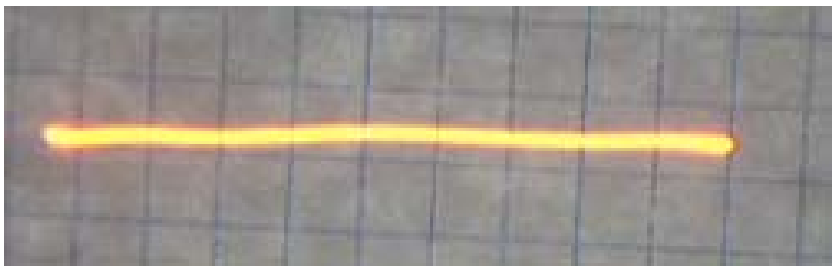

Figure 10: HeNe laser being scanned across a target using the prototype scanning devices..

Figure 11a is a picture of the ANSYS model used for the harmonic analysis. **Figure 11b** is a screen shot of the harmonic analysis animation. The results of the analysis can be seen in **Figure 12**. From the graph it is easy to see that the largest displacements of the mirror occur at approximately 24Hz, which correspond closely to actual measured resonant frequencies in prototype devices with the same dimensions.

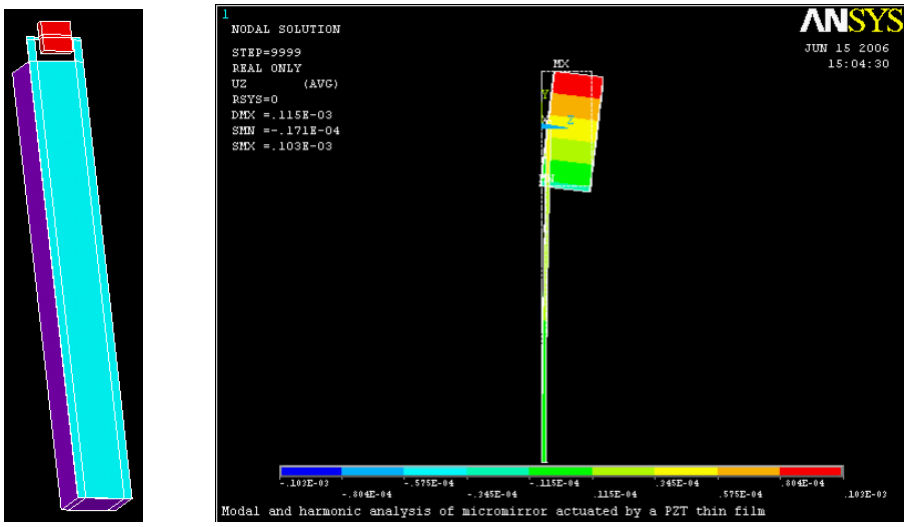

11a 11b

Figure 11: (a) Device used for ANSYS harmonic analysis of a 135um wide hinge (3um thick, 250um long) device with 1.5mm mirror attached. The different colors represent different materials. Red – gold plated silicon, blue-polyimide, purple-PZT. (b) Screen shot of the ANSYS harmonic analysis animation.

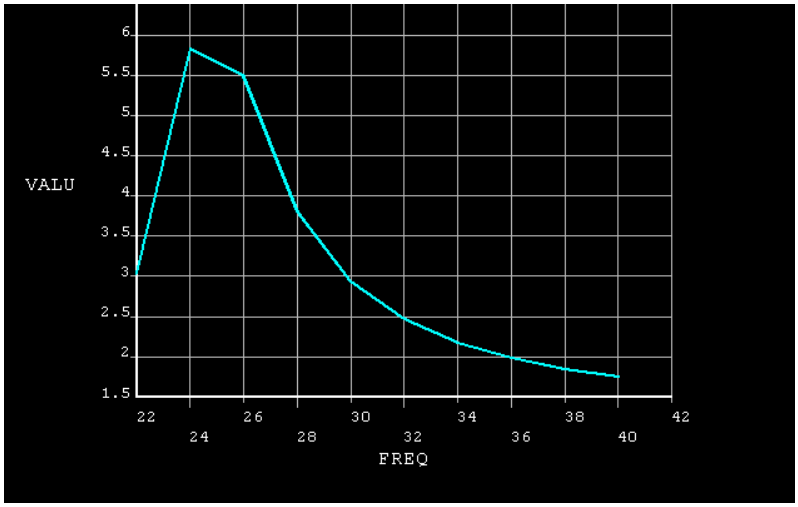

Figure 12: ANSYS harmonic analysis of a 135um hinge device with 1.5mm mirror attached.

3. **Fabrication**

Based upon the refined FEM and analytical models several new designs were selected for single wafer fabrication. The parametric variations in the new designs include different hinge thicknesses, mirror sizes, and cantilever actuators. Actuators of 1mm, 2mm, and 3mm lengths were chosen. Multiple cantilever actuators on a single device are also being designed. In previous prototype scanners only 75% of the scan was usable due to nonlinearities at the edges of the scans. With multiple cantilevers being used to drive a single device it will be possible to obtain a more linear scan from the device. The masks for the different cantilever designs can be seen in **Figure 13**.

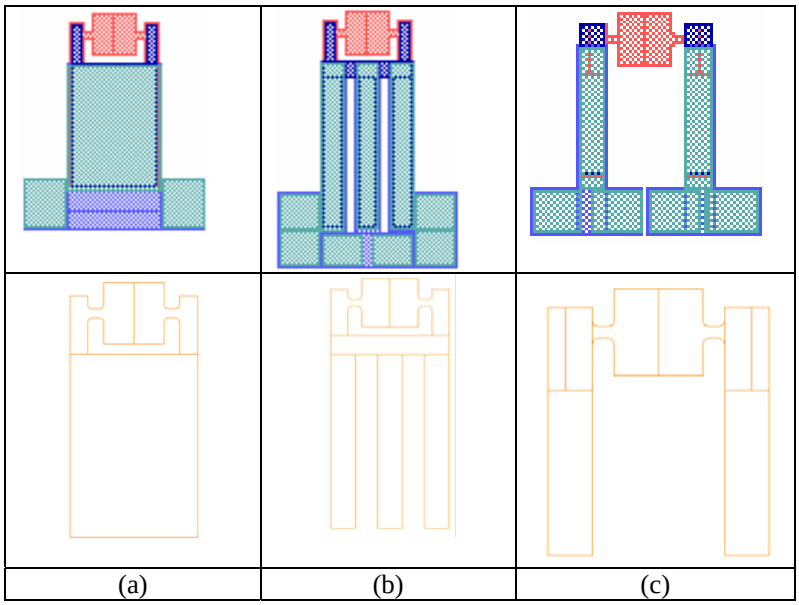

Figure 13: (a) Mask layout for single cantilever design, (b) Mask layout for triple cantilever design, (c) Mask layout for double cantilever design

The devices will be fabricated on a single four inch (450μm thick) test grade wafer with both sides being polished. The first step in the fabrication process is the growth of an oxide layer on the wafer. The oxide layer will serve as an etch stop for a later DRIE process. The oxide will also assist with the polyimide adhesion to the silicon. Following the oxide process step, TiPt will be deposited via sputter deposition. This will serve as the bottom electrode for the piezoelectric cantilever beam. The next step involves the deposition of the PZT layer. This will be done using a SolGel process. After the PZT is deposited the top electrode will be deposited using sputter deposition in the same manner as the bottom electrode. The top electrode layer will then be patterned using an ion mill. The ion mill will etch back to the PZT layer. The PZT layer, bottom electrode, and oxide will then be etched using the ion mill again. Following the ion mill etch of the cantilever, the PZT layer will be etched using a wet etch to expose the bottom electrode bonding pad. An oxide etch will then be done to remove the oxide from the location on the wafer where the polyimide hinges will be deposited. This is to ensure the hinge stiffness is not affected by the oxide. An oxide on the thin polyimide hinge can affect the device performance. The first polyimide layer (3μm thick) will then be spun on. The polyimide will then be patterned. This polyimide layer is the hinge layer for the device. A second polyimide layer (300μm thick) will be spun on to serve as the support structure. This layer will also be patterned like the first polyimide layer. The next process step involves a TiAu liftoff for the front side bonding pads as well as the backside mirror surface. The final step involves a backside DRIE process to remove the silicon wafer from underneath the area of the PZT cantilever beam and polyimide structure.

3. Conclusions

We have modeled and tested existing prototype scanning devices. The measurements from current prototypes allowed us to refine the existing FEM and analytical models. From these new models several new designs were chosen for fabrication. The mask layouts were done using AutoCad Lite. The masks have been fabricated and the devices are currently being fabricated. Future work includes the characterization and packaging of the new prototype devices as well as the characterization of thin film polyimide. The results from our modeling of the device have shown the devices capable of optical scan angles of up to 90 degrees using applied voltages of 5-50 V at frequencies of 15-50Hz. These figures show that this device is appropriate for real time imaging. The small size of the device and the large optical scan angles that it can achieve make this device ideally suited for use in various imaging system configurations, including minimally invasive medical imaging using endoscopy. The use of PZT and polyimide in actuators may also be of use in applications other than imaging.

References

[1] **"**New Opportunities for Optical MEMS are emerging outside of Telecom, says new CIR report - Market Intelligence - Communications Industry Researchers Inc", Fiber Optics Weekly Update, 7 March 2003.

[2] Z F Wang *et al* "Development of scanning micromirror with discrete steering angles" *Journal of Physics: Conference Series* **34** 410-416 (2006).

[3]Y S Yoon *et al* "A low voltage actuated micromirror with an extra vertical electrode for 90° rotation" *J. Micromech. Microeng.* **13** 922-926 (2003).

[4] Zhou, LX, Kahn, JM, Pister, KSJ "Scanning micromirrors fabricated by an SOI/SOI wafer-bonding process**"** J MICROELECTROMECH S 15 (1): 24-32 FEB 2006

[5] Johannes G Smits, Koji Fujimoto, and Vladimir Kleptsyn, "Microelectromechanical flexure PZT actated optical scanner: static and resonance behavior", J. Micromech. Microeng. 15(2005) 1285-1293.

[6] Chang-Hyeon Ji et al "An alectrostatic Scanning Micromirror with Diaphragm Mirror Plate and Diamond Shaped Reinforcement Frame," *J. Micromech. Microeng.* **16** 1033-1039 (2006).

[7] J. Zara and S. Smith, "Optical Scanner Using a Micromachine Actuator", *Sensors and Actuators: A: Physical*, 102 (1-2), pp. 176-184, 2002.

[8] Zara, J., S. Yazdanfar, K. Rao, J. Izatt and S. Smith, "Electrostatic MEMS Actuator Scanning Mirror for Optical Coherence Tomography," *Optics Letters*, 28(8), pp. 628-630, 2003.

[9] K.E. Petersen, "Silicon Torsional Scanning Mirror", IBM Journal of Research and Development **24**, 631-637 (1980)

[10] Yong-Hwa Park, K. C. Park "High-Fidelity Modeling of MEMS Resonators—Part II: Coupled Beam-Substrate Dynamics and Validation", JOURNAL OF MICROELECTROMECHANICAL SYSTEMS, VOL. 13, NO. 2, APRIL 2004